

magnetic branch of the equation of state, Eq. (17), one sees that this is the end point ($m \rightarrow 0$) of this branch. Hence the divergence occurs precisely at the second-order transition point. For temperatures $T < T_{12}$ the end point $m = 0$ is masked by the Maxwell construction. For $T > T_c$ there is no divergence.

The conclusion is thus that the γ -expansion result signals the onset of the phase transition to antiferromagnetic ordering. Although the transition occurs in zeroth order in γ , the signal comes from divergences in higher-order terms. It is

also worth noting that transitions are not necessarily determined by the total strength $\sum \varphi(n)$ of the attraction, the main factor in the ferromagnetic transition. For the present transitions the important factor is the periodic components in $\varphi(n)$.

ACKNOWLEDGMENT

The author wishes to thank Professor P. C. Hemmer for advice and help and discussion of problems and aspects concerning the model.

¹P. C. Hemmer and G. Stell, Phys. Rev. Letters 24, 1284 (1970); G. Stell and P. C. Hemmer, J. Chem. Phys. 56, 4274 (1972); W. K. Theumann and J. S. Høy, *ibid.* 55, 4159 (1971); J. F. Nagle, Phys. Rev. A 2, 2124 (1970); J. F. Nagle and J. C. Bonner, J. Chem.

Phys. 54, 729 (1971).

²J. L. Lebowitz and O. Penrose, J. Math. Phys. 7, 98 (1966).

³J. S. Høy (unpublished).

⁴P. C. Hemmer, J. Math. Phys. 5, 75 (1964).

PHYSICAL REVIEW B

VOLUME 6, NUMBER 11

1 DECEMBER 1972

New Mössbauer-Effect Measurements on ^{57}Fe in a Ni Host: The Critical Exponent β for Ni[†]

H. C. Benski* and R. C. Reno‡

Department of Physics, Brandeis University, Waltham, Massachusetts 02154

and

C. Hohenemser and R. Lyons§

Department of Physics, Clark University, Worcester, Massachusetts 01610

and

C. Abeledo¶

Department of Chemistry, Brandeis University, Waltham, Massachusetts 02154

(Received 28 February 1972; revised manuscript received 4 August 1972)

We have made new Mössbauer-effect measurements on Ni^{57}Fe in order to determine whether the results of Howard, Dunlap, and Dash in the critical region can be reproduced. We have used a longitudinally magnetized source foil in order to suppress the $\Delta m = 0$ hyperfine components, and have in this way increased our sensitivity near T_c by a factor of 5. We find that $\beta = 0.378 \pm 0.010$ for $3 \times 10^{-4} \leq 1 - T/T_c \leq 4 \times 10^{-2}$, with no indication of the double-valued behavior seen by Howard *et al.* Our result is in excellent agreement with recent perturbed-angular-correlation measurements on Ni^{100}Rh by our group, as well as previous determinations of β using a scaling equation of state. With the present work, it is possible to assert that all double-valued results for β in Ni have either been withdrawn or placed in serious doubt by subsequent work, and that the remaining experimental results cluster closely around $\beta = 0.38$, in good agreement with static scaling laws.

I. INTRODUCTION

For ferromagnets, the temperature dependence of the spontaneous magnetization in the vicinity of the critical temperature T_c has customarily been written

$$M_s(T) = B(1 - T/T_c)^\beta. \quad (1)$$

At the present stage of theoretical and experimental development, the critical exponent β is expected to be consistent with the scaling hypothesis, and

at least approximately consistent with calculable models such as the three-dimensional isotropic Heisenberg model.¹

For Ni, various determinations of β have been available for some time. These may be crudely divided into "direct" and "indirect" determinations. By "direct" we refer to methods in which the spontaneous magnetization

$$M_s(T) = \lim_{H \rightarrow 0} M(H, T) \quad (2)$$

is obtained from observations made with truly zero or quasizero applied fields H (corrected for demagnetization). By "indirect" we refer to methods in which the behavior of $M_s(T)$ is *deduced* from the behavior of $M(H, T)$ for appreciable values of the applied field H . An example of a "direct" experiment is a measurement of the hyperfine field H_{hf} in zero applied field, provided that

$$M_s(T) \propto H_{\text{hf}}(T). \quad (3)$$

An example of an indirect experiment is the measurement of the bulk magnetization, in which β is deduced as the value of a free parameter which best fits the observations of $M(H, T)$ using a scaling equation of state. The distinction between direct and indirect is somewhat ambiguous, to be sure. The kink-point bulk technique, for example, depends on appreciable applied fields for obtaining values of $M(H, T)$ above and below T_c , but then determines $M_s(T)$ directly from the trajectory of kink points observed for various applied fields.

At the time the present work was undertaken, the experimental situation for Ni was as follows.

Several authors had shown that scaling equations of state could be used successfully in fitting bulk measurements of $M(H, T)$; from these, they had obtained several independent values of β in the neighborhood of ~ 0.38 .²⁻⁵

Three "direct" experiments existed in which $M_s(T)$, in contrast to the above bulk measurements, *could not be described in terms of a single value of β* . In all three direct experiments, the numerical value of β was in agreement with scaling-equation-of-state fits only for temperatures far from T_c , and approached the classical value of $\beta = \frac{1}{2}$ close to T_c . Thus, given the correctness of bulk determinations of γ and δ , all three experiments were in violation of static scaling laws. The first of these experiments was a hyperfine-field measurement using the Mössbauer effect in Ni^{57}Fe , and was reported by Howard, Dunlap, and Dash⁶; the second was a neutron-depolarization measurement by Bakker, Rekveldt, and Van Loef⁷; and the third was a kink-point measurement by Arajs, Tehan, Anderson, and Stelmach.⁸

Recently, a "direct" measurement using perturbed angular correlations in Ni^{100}Rh showed that the hyperfine field could be fitted by a single value of β down to $1 - T/T_c = 10^{-4}$. This experiment, performed by Reno and Hohenemser,⁹ yielded $\beta = 0.385 \pm 0.005$, in good agreement with scaling-equation-of-state fits. It therefore stands in marked contrast to the other "direct" experiments discussed above.

It was tempting to attribute the observed discrepancies to errors made in determining T_c , or some other matter of instrumentation or data analysis. While such explanations turned out to be correct

in some cases (see below), the possibility remained that some of the observed discrepancies are real. If, for example, as was suggested to us by Dash,¹⁰ the difference in impurity-host coupling for Ni^{57}Fe and Ni^{100}Rh is the cause of the observed difference in critical behavior, serious consequences would follow; for this would mean that the condition expressed by Eq. (3) is *invalid*. That, in turn, means that no impurity hyperfine probe is a reliable measure of $M_s(T)$. It also would suggest that the phenomenological theory of impurity-host coupling developed by Jaccarino, Walker, and Wertheim,¹¹ and extended by Shirley, Rosenblum, and Matthias,¹² is invalid, for according to this theory, $H_{\text{hf}}(T)$ should approach $M_s(T)$ in the critical region even if there are measurable differences far from the critical point.

It seemed, therefore, worthwhile to reexamine the experimental basis for the apparent discrepancy between Ni^{57}Fe and Ni^{100}Rh in the critical region. Having just completed the work on Ni^{100}Rh , we turned our attention to Ni^{57}Fe .

After incorporation of essential improvements in the Mössbauer technique, we can report that a single value of β is now found to fit the range $3 \times 10^{-4} \leq 1 - T/T_c \leq 4 \times 10^{-2}$, and that numerically this value agrees within experimental error with the work on Ni^{100}Rh , as well as various scaling-equations-of-state determinations.

With our new data on Ni^{57}Fe , it appears that details of impurity-host coupling are eliminated as a major concern in hyperfine-field studies of static critical phenomena. The meaning of the new Mössbauer results in Ni^{57}Fe in the context of impurity-host coupling theories will be discussed elsewhere.¹³

While the present work was in progress, the following additional information became available.

Miyatani¹⁴ found in his kink-point experiment on Ni that a single value, $\beta = 0.398 \pm 0.010$, fits his data, in contrast to the work of Arajs *et al.*⁸ Except for the quoted number, no experimental details are given.

Gumprecht, Steiner, Crecelius, and Hufner¹⁵ in Mössbauer experiments on Ni^{57}Fe reported a single value of $\beta = 0.38 \pm 0.01$. Again, except for the quoted number, no details are given.

Anderson, Arajs, Stelmach, Tehan, and Yao¹⁶ reported that a careful reexamination of their earlier work revealed an erroneous determination of T_c , and that new measurements on the same Ni sample at very low applied fields and with a correct extrapolation to T_c yielded a single value of $\beta = 0.346 \pm 0.007$.

In Table I, we have summarized for convenience all experiments to date in which one or more of critical exponents β , γ , and δ has been determined for Ni.

TABLE I. Static critical exponents for Ni, summary of experimental results.

β	γ	δ	Applied field (kG)	Ref. ^a	Comments
	1.35 ± 0.02		0.05-18	b	Reanalysis of Weiss-Forrer ^g bulk data
	1.29 ± 0.03		0.04-0.36	c	Bulk data
0.51 ± 0.04^d			0	6	$Ni^{57}Fe$, H_{hf} , Mössbauer effect
0.33 ± 0.03^e					
0.41 ± 0.04	1.30 ± 0.05	4.22 ± 0.03	0.05-18	2	SES ^f reanalysis of Weiss-Forrer ^g data
0.3864	1.31 ± 0.01		0.05-18	3	SES ^f reanalysis of Weiss-Forrer ^g and new bulk data
0.378 ± 0.004	1.34 ± 0.01	4.58 ± 0.05	0.5-25	4	SES ^f analysis of new bulk data
0.50 ± 0.02			0	7	Neutron depolarization
0.375 ± 0.013	1.31 ± 0.01	4.48 ± 0.14	0.05-18	5	SES ^f reanalysis of Ref. 4 data
0.50 ± 0.01^d					
0.34 ± 0.01^e	1.31 ± 0.01	4.17 ± 0.05	0.008-1.1	8	Bulk data, kink-point technique
0.398 ± 0.010				14	Bulk data, kink-point technique
0.385 ± 0.005			0.002	9	$Ni^{100}Rh$, perturbed angular correlation
0.38 ± 0.01			0	15	$Ni^{57}Fe$, H_{hf} , Mössbauer effect
0.346 ± 0.007			0.003-0.095	16	Reanalysis of Ref. 8, new kink-point data
0.378 ± 0.010			0.001	This work	$Ni^{57}Fe$, H_{hf} , Mössbauer effect

^aLetter references refer to table footnotes, number references to text.

^bJ. S. Kouvel and M. E. Fisher, Phys. Rev. **136**, A1626 (1964).

^cS. Aaraj, J. Appl. Phys. **36**, 1136 (1967).

^dFor $10^{-4} < 1 - T/T_c < 9 \times 10^{-3}$.

^eFor $9 \times 10^{-3} < 1 - T/T_c < 10^{-1}$.

^fSES is the abbreviation for scaling equation of state.

^gReference 29.

II. TECHNICAL IMPROVEMENTS

In addition to the experiments on $Ni^{57}Fe$ discussed above,^{6,15} there have been several other previous Mössbauer experiments in which the critical exponent β has been determined from the hyperfine splitting.¹⁷⁻¹⁹ Except for the work of Wertheim on FeF_2 and FeF_3 , all previous work suffered from serious lack of resolution in the region $10^{-4} \leq 1 - T/T_c \leq 10^{-3}$; and in all cases, the cause for this was the fundamental linewidth of Mössbauer-hyperfine components. This situation led to a choice between two equally unpleasant alternatives: (i) interpretation of unresolved spectra without sufficient information on possible hidden effects, such as line broadening near T_c ; or (ii) elimination of unresolved data from the experiment. Howard *et al.*⁶ chose the first of these alternatives, and most other authors chose the second. In the case of Groll's study of EuO ,¹⁹ the effect of the second alternative is particularly severe in that resolved spectra were limited to $1 - T/T_c \geq 1.4 \times 10^{-2}$.

A. Source Polarization

In the work reported here, the unpleasant choice described above was circumvented. Resolution of hyperfine spectra near T_c was markedly increased by use of a source foil that was magnetized in a direction nearly parallel to the axis of γ -ray detection. In this way, the well-known²⁰ suppres-

sion of $\Delta m = 0$ Zeeman components is induced, and the intensity of the outermost and innermost lines is increased. To see this in more detail, consider the experimental geometry shown in Fig. 1. The source foil is clamped between the pole pieces of a small C-type electromagnet, and the acceptance angle of the detector is between 10° and 22° with respect to the axis of magnetization. If we label the outer, intermediate, and inner lines by (1, 6), (2, 5), and (3, 4) in the usual manner, we may derive the following intensity ratios. For zero magnetization, $I_{1,6} : I_{2,5} : I_{3,4} = 3 : 2 : 1$. For complete magnetization and detection *exactly* along the direction of magnetization, $I_{1,6} : I_{2,5} : I_{3,4} = 3 : 0 : 1$.

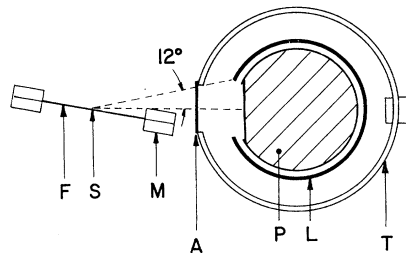


FIG. 1. Diagram of the source-counter geometry drawn to scale. F, source foil; S, source; M, magnet yoke; A, resonant absorber; P, proportional counter; L, lead shield; and T, Lucite ring attached to velocity transducer.

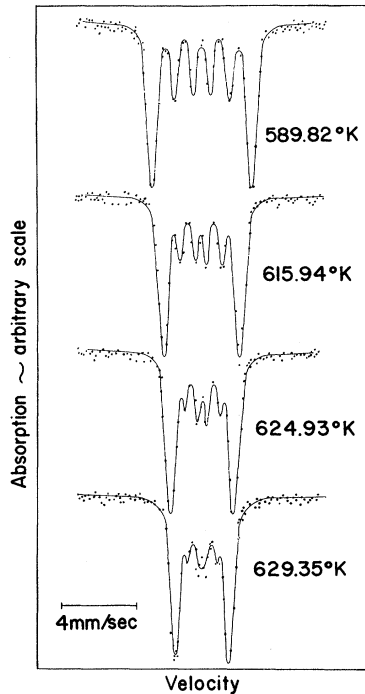


FIG. 2. Series of spectra taken with a 5-G applied field, indicating the suppression of the $\Delta m = 0$ components as T_c is approached.

For complete magnetization, and detection as in the experimental geometry, $I_{1,6} : I_{2,5} : I_{3,4} = 3 : \frac{1}{6} : 1$.

The remaining question is whether conditions of complete magnetization can be obtained in the critical region. For the study of ferromagnetic critical points it is, of course, crucial that applied magnetic fields be nearly zero, since otherwise the limit expressed in Eq. (2) is violated. In the present work, it was found that an appreciable field (~ 200 G) is needed to saturate the source foil far below T_c ; as T_c is approached, fields needed to saturate the source foil decrease markedly. This observation is entirely consistent with a simi-

TABLE II. Summary of sensitivity of Mössbauer critical-point studies in $Ni^{52}\text{Fe}$.

Experiment	Error in Curie temp. $\Delta T_c/T_c$	Resolved spectra $(1 - T/T_c)_{\min}$
Howard <i>et al.</i> ^a	1.5×10^{-4}	10^{-2}
Gumprecht <i>et al.</i> ^b
This work	10^{-4}	3×10^{-4} ^c 10^{-2} ^d

^aReference 6.

^bReference 15.

^cLine structure visible, but curve fitting necessary to extract H_{hf} .

^dLine structure resolved, no fitting necessary to extract H_{hf} .

lar finding by Reno and Hohenemser^{9,21} in perturbed-angular-correlation experiments in $Ni^{100}\text{Rh}$. Both observations may be attributed to a combination of well-known factors; in particular, a decrease of the anisotropy field as T_c is approached,²² and a decrease of the demagnetizing field as T_c is approached.

Experimentally, the degree of source magnetization may be studied through direct observations on Mössbauer spectra. To illustrate this, Fig. 2 shows a series of spectra taken with increasing temperature and an applied field of 5 G. The gradual suppression of the intensity $I_{2,5}$ is clearly evident. In Fig. 3, a summary of data for the line intensity ratio $I_{2,5}/I_{1,6}$ is given as a function of temperature and applied field. From this it is seen that in a region extending $\sim 5^\circ\text{K}$ below T_c , the intensity ratio approaches the value expected for complete magnetization, even if the applied field is as small as 1 G. (The intensities were derived from curve-fitting procedures described below.)

Reno and Hohenemser have shown experimentally that applied fields of 1–2 G do not lead to detectable rounding of H_{hf} for $1 - T/T_c \geq 10^{-4}$. A similar conclusion may be reached by use of a scaling equation of state. In the present work, applied fields of 1 G were used to the last interpretable point at $1 - T/T_c = 3.0 \times 10^{-4}$ without correction for critical-point rounding.

The benefits realized through the use of a longitudinally polarized source may be characterized by two criteria: (i) the minimum reduced temperature for which the hyperfine spectrum is resolved; and (ii) the fractional error in T_c as determined self-consistently from the data. In Table II, all critical-point studies on $Ni^{57}\text{Fe}$, including the present

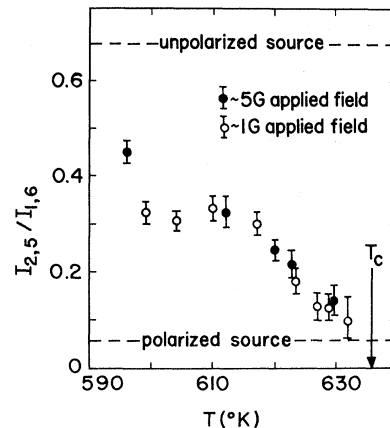


FIG. 3. Temperature dependence of $I_{2,5}/I_{1,6}$ for applied fields of 1 G (open circles) and 5 G (closed circles). The ratios were obtained with the curve-fitting procedure described in the text, and include only spectra for which unique six-line fits could be made.

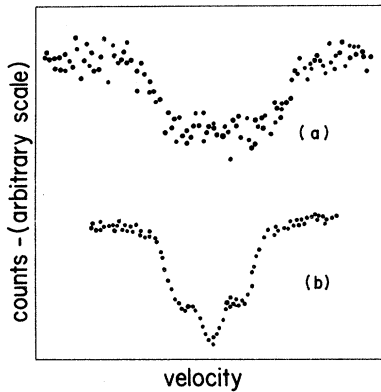


FIG. 4. Illustration of improved statistics in the present study: comparison of two spectra taken at 0.7°K below T_c by Howard *et al.* (top) and in this work (bottom). The difference in general shape is due to our suppression of the $\Delta m = 0$ components.

work, are compared with respect to these two criteria.

B. Improved Counting Statistics

In addition to line suppression, counting statistics were optimized in the present work for obvious reasons. This surprisingly was not a trivial matter, and led to a series of interdependent requirements as follows.

(i) Near T_c , the dip size of the outer lines is maximally $\sim 4\%$ because of a reduced recoilless fraction and nonresonant absorption. For "good" statistics, which we consider to be characterized by a 40:1 signal-to-noise ratio, about 10^6 counts per channel are required.

(ii) Impurity concentration in the source should be well below 0.1 at. % if impurity-impurity interactions are to be avoided.

(iii) For a source-counter geometry that provided sufficient space for the polarizing magnet, requirement (ii) implies a maximum source strength of ~ 1 mC.

(iv) Taken together, requirements (i) and (iii) imply a counting time of 24–48 h/point, with concomitant temperature stability. A comparison of statistics obtained in the present work and the earlier study by Howard *et al.*⁶ is seen in Fig. 4.

C. Temperature Control

The temperature-control system used was similar to that developed by Reno.²¹ It employed a heater and two thermocouples, one for measuring and one for feedback control. The thermocouples probe consisted of a BeO disk 0.05 cm thick in which the thermocouples were embedded. The disk was sandwiched with the source foil between two thicker disks on which the heater was wound. The entire assembly was clamped by a stainless-steel

clamp and surrounded by an asbestos cover.

The two thermocouples were spaced by 0.6 cm and exhibited temperature differences no greater than 0.2°K . Since the source was 0.1 cm in diameter we conclude that the source temperature inhomogeneity was less than 0.03°K . Specifications for the temperature-control system are given in Table III.

III. ANALYSIS OF SPECTRA

The spectra obtained in this experiment can be roughly divided into two classes: (i) well resolved and (ii) partially resolved. For the well-resolved spectra, the splitting $\Delta_{1,6}$ of lines 1 and 6 can be read from a plot without appreciable error, although curve fitting is necessary to extract reliable values of the intensities and linewidths. For the partially resolved spectra, though structure is clearly evident, derivation of the splitting requires curve fitting as well. The division between the two classes lies at about $(1 - T/T_c) = 10^{-2}$.

A. "Signature" of Partially Resolved Spectra

Before turning to the details of our curve-fitting procedures, we may indicate briefly the qualitative

TABLE III. Specifications of the Mössbauer apparatus.

1. Source foil	
Material:	99.998%-pure Ni
Dimensions:	0.0025 cm thick
^{57}Co activity:	1.5 mCi, near uniform distribution
^{57}Co atomic concentration:	10^{-4}
Diffusion conditions:	30 h, 1150°C , in H_2
2. Resonant absorber	
Material:	90 at. % ^{57}Fe enriched $\text{K}_4\text{Fe}(\text{CN})_6 \cdot 3\text{H}_2\text{O}$
Thickness:	0.25 mg/cm^2 of ^{57}Fe
3. Nonresonant absorbers	
Heater window:	BeO, 0.050 cm
Heater cover:	asbestos-base paper, 0.020 cm
Absorber matrix:	Lucite, 0.15 cm
Absorber:	2 mg/cm^2 of $\text{K}_4\text{Fe}(\text{CN})_6 \cdot 3\text{H}_2\text{O}$ less ^{57}Fe
Proportional counter window:	Be, 0.025 cm
4. Magnet	
Type:	C yoke, armco iron, clamping foil in closed magnetic circuit
Field:	0–210 G
Gap:	4.4 cm
Field monitoring:	Hall-probe gaussmeter
5. Geometry	
Source to counter distance:	6.25 cm
Counter aperture:	2.5 cm
Acceptance angle:	10° – 22° with respect to source foil magnetization
6. Temperature control	
Short-term instability (24 h):	0.02°K
Long-term instability (several days):	0.05°K
Thermocouple type:	chromel constantan, 0.025 mm diam
Potentiometer sensitivity:	$1 \mu\text{V}$, or 0.012°K

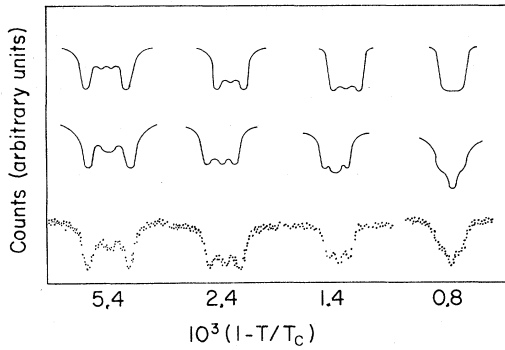


FIG. 5. Signature of partially resolved spectra. Top row, assuming that linewidth is independent of temperature and velocity; second row, assuming that linewidth varies with temperature as described in the text; bottom row, experimental data of this study.

aspects of partially resolved spectra under various assumptions.

(a) *Constant linewidth throughout.* Howard *et al.*⁶ assumed that the linewidth did not vary with temperature. Under this assumption, a sequence of increasingly collapsed spectra, using the line intensities appropriate for the present work, would appear as shown in Fig. 5, line 1. No central maximum occurs at any point during the collapse.

(b) *Line broadening near T_c .* If one assumes that below $(1 - T/T_c) = 10^{-2}$ the linewidth of each line increases such that the excess width is proportional to $(1 - T/T_c)^{1/2}$ and the excess of a particular pair of lines is proportional to the velocity of that pair, we obtain results as shown in Fig. 5, line 2.

For the calculated spectra above, we have chosen values of $\Delta_{1,6}$ that correspond to those of available experimental data. These data are shown in Fig. 5, line 3. From these, we draw the following conclusions.

(i) The assumption of constant linewidth made in Ref. 6 leads to spectra in the partially resolved region that are *qualitatively different* from our data.

(ii) The assumption of divergent linewidth described in (b) above leads to spectra that are in *qualitative agreement* with our data. A particularly interesting feature of the partially resolved spectra under assumption (b) is the emergence of the central "line" as T_c is approached. From our qualitative analysis, we conclude that this line is due to the coalescence of lines 3 and 4 and not to paramagnetic regions. The principal reason for this is that the central maximum maintains a roughly constant size as T_c is approached, and this size can be entirely explained by the superposition of discrete Zeeman components. For superparamagnetism, on the other hand, one would ex-

pect rapid growth of the central maximum at the expense of the rest of the spectrum.

In this regard, we note the close similarity between our spectra in the partially resolved region and those observed by Maletta, Rao, and Nowik²³ in Mo^{57}Fe . These authors, like ourselves, used a longitudinally polarized source, and then explained their results by relaxation effects superimposed on a *pure* Zeeman spectrum. We may also contrast our results with the work of Levinson, Luban, and Shtrikman²⁴ on ^{57}Fe in YFe_2O_3 and FeF_3 , who found near T_c that a central peak could not be interpreted in terms of pure Zeeman components, but required the presence of superparamagnetism.

B. Curve-Fitting Procedures

All spectra were fitted with a multiparameter least-squares program developed by Chrisman and Tumolillo²⁵ at the University of Illinois. The fits were constrained by symmetry requirements on linewidths and intensities as follows:

$$\Gamma_1/\Gamma_6 = \Gamma_2/\Gamma_5 = \Gamma_3/\Gamma_4 = 1, \quad (4)$$

$$I_1/I_6 = I_2/I_5 = I_3/I_4 = 1. \quad (5)$$

In addition, we required

$$I_1/I_3 = 3. \quad (6)$$

In the well-resolved region it was possible with these constraints to achieve excellent 13-parameter six-line fits to the data. The free parameters were the baseline and its slope, and six-line positions, I_1 , I_2 , Γ_1 , Γ_2 , and Γ_3 . As expected, the splittings obtained were nearly identical to those derived by graphical methods. In the partially resolved region, curve fitting reflected the rapidly decreasing intensity of lines 2 and 5 (see Fig. 3). For $10^{-2} < 1 - T/T_c < 10^{-3}$ reasonable six-line 13-parameter fits could be obtained; however, for $4 \times 10^{-3} < 1 - T/T_c < 10^{-3}$, equally good four-line nine-parameter fits were possible. The latter yielded values for the splitting $\Delta_{1,6}$ that were consistently lower by about 4% than the splitting obtained from the corresponding six-line fits. Typical data and their associated fits are shown in Fig. 6.

IV. LINEWIDTH

In order to understand our spectra as fully as possible, we made a study of linewidth as a function of temperature prior to the determination of β . The principal results of this study are described in Secs. IV A and IV B.

A. Instrumental Broadening

Well above T_c , outside the region of critical fluctuations, a single line of width 0.355 mm/sec was observed. To within 3%, this width could be

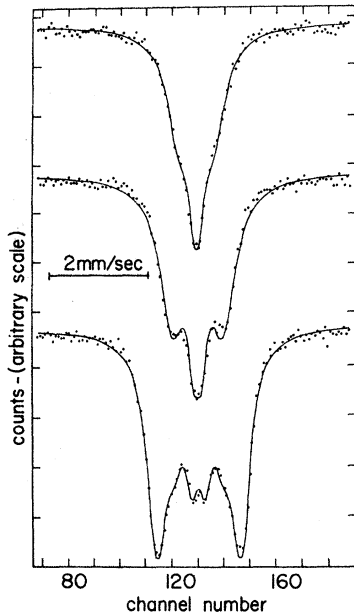


FIG. 6. Illustration of the quality of curve fitting obtained in this study. Spectra from top to bottom are for reduced temperatures of 3.0×10^{-4} , 1.18×10^{-3} , and 1.16×10^{-2} , respectively. The top two spectra are in the "close-in" region (see Table IV), and were fitted with four lines. The bottom is the first point in the "far-out" region, and was fitted with six lines.

accounted for by three well-known instrumental effects: (i) the finite thickness of the resonant absorber²⁶; (ii) the effect of finite channel resolution in the multichannel analyzer; and (iii) the effect of an additional $\frac{1}{2}$ channel uncertainty in the trigger time of the multichannel sweep when the spectrometer is run in the time mode. We are thus assured that at least at zero velocity, noninstrumental sources of line broadening are negligible.

For lines at finite velocity, one may expect some additional instrumental broadening and line shifting due to the finite acceptance angle of the moving absorber. By explicit calculation for our experimental geometry we have shown that this is about 0.02 mm/sec of the total width for lines occurring at maximum experimental velocities. The line shifts arising from finite absorber acceptance angle are proportional to velocity in first order, and do not exceed 1% of the line velocity. They also do not affect our results, since only *relative* variation of hyperfine splitting is of interest here.

B. Solid-State Effects

Given these instrumental effects, we define the excess width of a given line as

$$\Delta\Gamma = \Gamma - \Gamma_0. \quad (7)$$

Here Γ_0 is the width expected on instrumental

grounds and Γ is the measured width. Values of $\Delta\Gamma$ were derived from the least-squares analysis of the spectra. The results are plotted in Fig. 7 for lines 1 and 6. We draw the following conclusions.

(i) Far below T_c , the outer lines are approximately 20% broader than would be predicted on instrumental grounds. The cause of this broadening is unknown, but it is unlikely to be inhomogeneities, since the effect is temperature independent.

(ii) For a given temperature, the broadening increases with the velocity of the line. Because of the small splitting of the inner lines, a more quantitative conclusion is not possible.

(iii) For $1 - T/T_c < 10^{-2}$, $\Delta\Gamma$ increases by more than a factor 3. This linewidth anomaly occurs for a region in which Howard *et al.*⁶ could not obtain explicit fits to their data, and it was presumably missed by them for this reason. In contrast to the finding of Gumprecht *et al.*,¹⁵ the anomaly cannot be fit by a power law. In this way, the results are similar to the NMR data for FeF_2 ²⁷ and unlike the NMR data for MnF_2 .²⁸ The cause of the anomaly can lie in either static or time-dependent phenomena, i.e., field inhomogeneities or critical fluctuations. The anomaly cannot be attributed to the small temperature inhomogeneity in the source already alluded to.

V. RESULTS

In the course of the work, several series of runs were made in which Mössbauer spectra were taken as a function of temperature below T_c . In this way, we observed a slight deviation of the reduced hyperfine field from the reduced magnetization as measured by Weiss and Forrer.²⁹ The effect was similar to, though smaller, than the one observed by Dash, Dunlap, and Howard³⁰ and did not exceed 10% at any temperature. Since available models^{11,12} predict that the reduced field is proportional to the magnetization near T_c , the observed deviations are not further analyzed in the context of this paper.

In the following, we consider in detail a series of 19 points taken without interruption over a

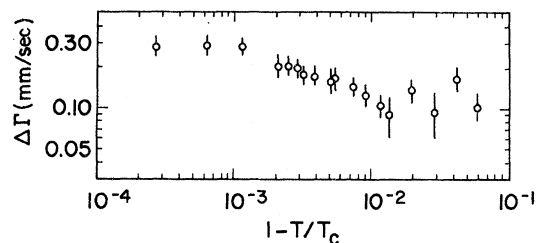


FIG. 7. Temperature dependence of the excess width $\Delta\Gamma$ for lines 1 and 6, as deduced from the curve-fitting procedures.

TABLE IV. Hyperfine splitting near T_c .

T (°K) ^a	$1 - T/T_c$ ^b	h^c	Chronol. order	Comments
635.76	3.0×10^{-4}	0.073 ± 0.005	7	"Close-in" region; spectra partially resolved; only four-line fits are possible.
635.53	6.6×10^{-4}	0.096 ± 0.005	5	
635.39	9.1×10^{-4}	0.102 ± 0.005	19	
635.20	1.18×10^{-3}	0.115 ± 0.005	3	
634.63	2.07×10^{-3}	0.151 ± 0.005	4	"Intermediate" region; spectra partially resolved; both four- and six-line fits are possible; six-line fits are chosen for numbers quoted here because they are better.
634.38	2.47×10^{-3}	0.161 ± 0.005	2	
634.23	2.71×10^{-3}	0.161 ± 0.005	6	
633.86	3.29×10^{-3}	0.183 ± 0.005	1	
633.35	4.08×10^{-3}	0.196 ± 0.005	10	
632.64	5.21×10^{-3}	0.214 ± 0.005	9	
631.46	7.06×10^{-3}	0.240 ± 0.005	11	
629.84	9.60×10^{-3}	0.271 ± 0.002	12	
628.59	1.16×10^{-2}	0.288 ± 0.002	13	
627.32	1.36×10^{-2}	0.309 ± 0.002	8	
623.54	1.95×10^{-2}	0.355 ± 0.002	14	"Far out" region; spectra are resolved; six-line fits in agreement with graphical methods of deducing the splitting.
617.83	2.85×10^{-2}	0.411 ± 0.002	15	
610.27	4.04×10^{-2}	0.469 ± 0.002	16	
597.69	6.01×10^{-2}	0.538 ± 0.002	17	
573.17	9.87×10^{-2}	0.630 ± 0.002	18	

^aRelative error in T : ± 0.02 °K; absolute error in T : ± 2 °K.

^bReduced temperature based on $T_c = 635.95 \pm 0.07$ °K.

^cError quoted for reduced field is approximately three times the statistical error of the curve fitting.

period of 37 days in the interval $3 \times 10^{-4} < 1 - T/T_c < 4 \times 10^{-2}$. The velocity calibration was based on the splitting observed for an Fe absorber at 300 °K, and the absolute determination of this splitting by Preston, Hanna, and Heberle.³¹

The results of our curve-fitting procedures are summarized in Table IV. As already mentioned, in the region $10^{-3} < 1 - T/T_c < 4 \times 10^{-3}$, both four- and six-line fits could be made to the spectra with equal success. This is not unreasonable, since in this region the intensity $I_{2,5}$ is approaching the value expected for a fully polarized source, and the structure of the spectra shows no visible evidence (peaks, inflection points) that can be attributed to lines 2 and 5. For Table IV, the splittings given by the six-line fits were chosen because they were somewhat better fits; at the same time, the quoted error in the splitting was arbitrarily increased to include in its range the results of the four-line fits.

The reduced fields $h = H_{\text{hf}}(T)/H_{\text{hf}}(0)$ given in Table IV were calculated by using $H_{\text{hf}}(0) = 283$ kG, obtained by extrapolating our room-temperature measurement to zero temperature.

As a check on the reproducibility of the temperature scale, the chronological order of the points, also given in Table IV, was arranged so that very similar splittings were measured at widely different times. Careful analysis of the data shows no inconsistencies, and we conclude that the temperature scale was stable. It is to be emphasized that

the temperature scale has no *absolute* significance since the thermocouples are not calibrated in the critical region.

To determine β , a fit to the form

$$h = B(1 - T/T_c)^\beta \quad (8)$$

was made in which B , T_c , and β were treated as parameters. Equation (8) was first linearized to

$$\begin{aligned} h^{1/\beta} &= (B^{1/\beta}/T_c)(T_c - T) \\ &= a + bT, \end{aligned} \quad (9)$$

and then the constants a and b were determined by least squares for various values of β . The least-squares error for a and b both took on minimum values in the neighborhood of $\beta = 0.378$, indicating that this β value gives the best fit.

To obtain an estimate of the uncertainty in β we used a graphical method first employed by Heller²⁸ and later by Wertheim¹⁷ and Reno and Hohenemser⁹ and others.

(i) For each of several values of β , plots of $\Delta T/T$ vs T are made, where $\Delta T/T$ are the fractional deviations of the data points from the "best line" of the form (9), as determined by least squares.

(ii) The range of β consistent with the data is then defined by the requirement that no statistically significant deviation from zero occurs in $\Delta T/T$ vs T .

From inspection of Fig. 8, we conclude that ac-

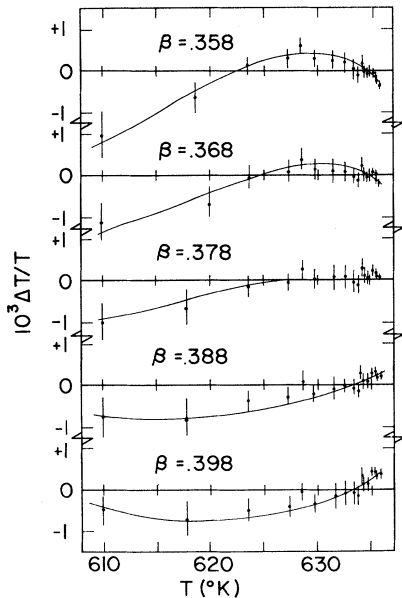


FIG. 8. Fractional deviations $\Delta T/T$ from the "best line" of the form $h^{1/\beta} = a + bT$ for various values of β . The error bars reflect the uncertainty in h as quoted in Table IV.

According to this criterion

$$\beta = 0.378 \pm 0.010, \quad (10)$$

$$3 \times 10^{-4} < 1 - T/T_c < 4 \times 10^{-2}.$$

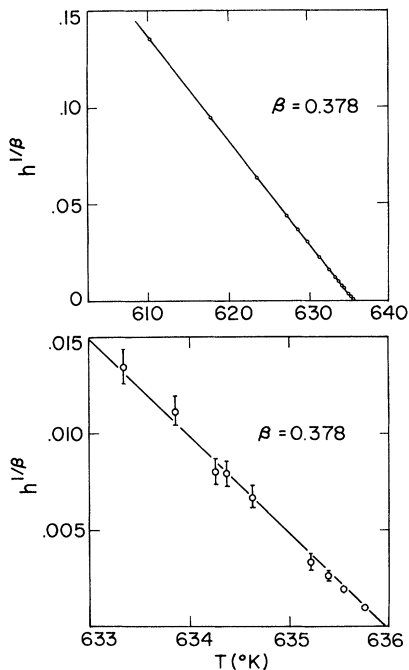


FIG. 9. Plot of $h^{1/\beta}$ vs T for the best value of β shown for two ranges of temperature. The continuous line represents the least-squares fit for $\beta = 0.378$.

For the region $1 - T/T_c > 4 \times 10^{-2}$ a consistent, albeit small, deviation from zero is observed in the $\Delta T/T$ plots for all values of β , indicating that in this region no power-law fit can be made that is consistent with the close-in region, no matter what value of β is chosen.

The range of β values defined above implies a range of values for the parameters a and b obtained by least-squares analysis, i. e.,

$$B = 1.56 \pm 0.06, \quad (11)$$

$$T_c = 635.97 \pm 0.12 \text{ }^\circ\text{K}. \quad (12)$$

It must be realized that the above value of T_c and its uncertainty are based on use of the 17 data points closest to the Curie temperature. These points include some which according to Fig. 8 indicate the breakdown of the power law at the low-temperature end of the experimental range. By eliminating eight points from the low-temperature end of the range, the result

$$T_c = 635.95 \pm 0.07 \text{ }^\circ\text{K} \quad (13)$$

is obtained.

As a graphical illustration of the quality of the data, our results are shown in the form $h^{1/\beta}$ vs T in Fig. 9 for two temperature ranges. Independent of any of our fitting procedures, Fig. 9 confirms the correctness of our choice of T_c .

A final way of presenting our results is the commonly used logarithmic plot, shown in Fig. 10. The horizontal error bars indicate the uncertainty in T_c . The dotted line approximates the behavior reported by Howard *et al.*⁶

VI. CONCLUSIONS

If the validity of the present experiment is accepted, the situation at this writing is that all double-valued results for β in Ni have either been withdrawn or placed in serious doubt by subsequent work. With the exception of the most recent kink-point measurement of Anderson *et al.*¹⁶ and the neutron-depolarization results of Bakker *et al.*,⁷ directly determined experimental β values cluster

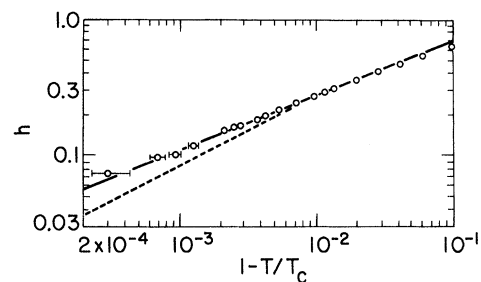


FIG. 10. Logarithmic plot of h vs $1 - T/T_c$, comparing this work (points) to the results of Ref. 6 (dashed line). Bars indicate error in T_c .

closely around 0.38. Taken together with experimental values of γ , α , and δ , this value of β leads to good agreement with indirect determinations obtained by scaling-equation-of-state fits to the magnetization.

In addition, the results of the present work suggest that the details of impurity-host coupling do not affect the usefulness of hyperfine-field measurements as probes of static critical phenomena—quite independent of theoretical considerations. The results of carefully conducted hyperfine-field

measurements in the critical region are not only in close agreement when different impurity atoms are used in the same host, but these experiments are also in agreement with the results of bulk measurements.

ACKNOWLEDGMENTS

We happily acknowledge several stimulating discussions with Peter Heller and Albert Gottlieb, and thank the latter for assistance with the computer analysis.

†Work supported in part by the U. S. Atomic Energy Commission and Research Corp.

*Present address: Institut de Physique Nucleaire, 91 Orsay, France.

‡Present address: National Bureau of Standards, Washington, D. C.

§Undergraduate research participant, Clark University.

¶Visiting scientist, Francis Bitter National Magnet Laboratory.

¹H. E. Stanley, *Introduction to Phase Transitions and Critical Phenomena* (Oxford U.P., New York, 1971).

²J. S. Kouvel and D. S. Rodbell, Phys. Rev. Letters **18**, 215 (1967).

³A. Arrott and J. E. Noakes, Phys. Rev. Letters **19**, 787 (1967).

⁴J. S. Kouvel and J. B. Comly, Phys. Rev. Letters **20**, 1237 (1968).

⁵M. Vicentini-Missoni, R. Joseph, M. Green, and J. L. Sengers, Phys. Rev. B **1**, 2312 (1970).

⁶D. G. Howard, B. D. Dunlap, and J. G. Dash, Phys. Rev. Letters **13**, 752 (1964).

⁷H. Bakker, M. Rekveldt, and J. Van Loef, Phys. Letters **27A**, 69 (1968).

⁸S. Arajs, B. Tehan, E. Anderson, and A. Stelmach, Phys. Status Solidi **41**, 639 (1970).

⁹R. C. Reno and C. Hohenemser, Phys. Rev. Letters **25**, 1007 (1970).

¹⁰J. G. Dash (private communication).

¹¹V. Jaccarino, L. R. Walker, and G. Wertheim, Phys. Rev. Letters **13**, 752 (1964).

¹²D. A. Shirley, S. S. Rosenblum, and E. Matthias, Phys. Rev. **170**, 363 (1968).

¹³C. Hohenemser, R. C. Reno, and H. C. Bensi (unpublished).

¹⁴K. Miyatani and K. Yoshikawa, J. Appl. Phys. **11**, 1272 (1970).

¹⁵D. Gumprecht, P. Steiner, G. Crecelius, and S. Hüfner, Phys. Letters **34A**, 79 (1971).

¹⁶E. Anderson, S. Arajs, A. Stelmach, B. Tehan, and Y. Yao, Phys. Letters **36A**, 173 (1971).

¹⁷G. K. Wertheim and H. J. Guggenheim, in *Hyperfine Structure and Nuclear Radiation*, edited by E. Matthias and D. A. Shirley (North-Holland, Amsterdam, 1968), p. 531.

¹⁸R. Preston, J. Appl. Phys. **39**, 1231 (1968).

¹⁹G. Groll, Z. Physik **243**, 60 (1971).

²⁰H. Frauenfelder, D. Nagle, R. Taylor, D. Cochran, and W. Visscher, Phys. Rev. **126**, 1065 (1961).

²¹R. C. Reno, dissertation (Brandeis University, 1970) (unpublished).

²²D. S. Rodbell, Physics **1**, 279 (1965).

²³H. Maletta, K. R. P. M. Rao, and I. Nowik, Z. Physik **249**, 189 (1972).

²⁴L. M. Levinson, M. Luban, and S. Shtrikman, Phys. Rev. **177**, 864 (1969).

²⁵B. L. Chrisman and T. A. Tumolillo, Tech. Rept. No. 178, NSF Grant No. GP-9311 (University of Illinois, Urbana, 1969) (unpublished).

²⁶S. Margulies and J. R. Ehrmann, Nucl. Instr. **12**, 131 (1961).

²⁷S. Kulpa, dissertation (Brandeis University, 1967) (unpublished).

²⁸P. Heller and G. Benedek, Phys. Rev. Letters **8**, 428 (1962); also P. Heller, dissertation (Harvard University, 1962) (unpublished).

²⁹P. Weiss and R. Forrer, Ann. Phys. (Paris) **5**, 153 (1926).

³⁰J. G. Dash, B. D. Dunlap, and D. G. Howard, Phys. Rev. **141**, 376 (1965).

³¹R. Preston, S. S. Hanna, and J. Heberle, Phys. Rev. **128**, 2207 (1962).